

Synthesis and investigation of langbeinite-related strontium- and iron-containing phosphates

Nataliia STRUTYNSKA*^{ORCID}, Nikolai SLOBODYANIK^{ORCID}, Anastasiia SHATALOVA^{ORCID}
Department of Chemistry, Taras Shevchenko National University of Kyiv, Kyiv, Ukraine

Received: 11.07.2017

Accepted/Published Online: 17.07.2018

Final Version: 06.12.2018

Abstract: The partial substitution of potassium atoms by strontium atoms in initial matrix $K_3Fe_2(PO_4)_3$ with formation of complex phosphates $K_{3-2x}Sr_xFe_2(PO_4)_3$ ($x = 0.75, 1.0, \text{ and } 1.25$) was determined using a solid-state reaction method. According to powder X-ray diffraction (XRD) data, the prepared phosphates with $x = 1.0$ and 1.25 crystallize in a cubic system (space group $P2_13$) and belong to langbeinite family compounds, while for the sample with $x = 0.75$ a mixture of langbeinite-type phase and a minor amount of $K_3Fe_2(PO_4)_3$ was obtained. The decreasing trend of lattice parameter a with increase of Sr amount in the phosphate confirmed the incorporation of strontium in the langbeinite-related structure. The thermal analysis results indicate that the obtained langbeinite-related compounds are stable upon heating and their melting points are higher than $1000^\circ C$. It should be noted that the determined iron-containing phosphates can be obtained at temperature lower than $900^\circ C$, which creates a perspective for using them as matrixes for immobilization of radioactive strontium.

Key words: Langbeinite, X-ray diffraction, phosphate, strontium, thermogravimetry/differential thermal analysis

1. Introduction

One of the most crucial aspects linked to nuclear power is the disposal of radioactive waste. The strontium isotope ^{90}Sr (with relatively long half-life of roughly 29 years) is a typical high-level radioactive component, the wastes of which are treated as one of the most dangerous products of nuclear fission for human beings.¹ Currently, many methods have been proposed for stabilization of radioactive ions. The first one is to use ionic exchangers for purification and volume reduction of liquid radioactive wastes, such as chabazite² and natural zeolites.^{3–5} An alternative way is applying waste immobilization technologies that involve producing glass or ceramic compounds with enhanced chemical and thermal stability with respect to the leachability of ions in water and aggressive media. In this aspect, borosilicate,^{6,7} phosphate glasses,^{8–11} and ceramic mineral-like substances such as apatite,^{12,13} monazite,^{14–18} whitlockite,¹⁹ NZP $NaZr_2(PO_4)_3$,^{20–28} langbeinite,^{29,30} and others^{31,32} have been studied. Among them, the complex phosphates with NZP type structure $(NaZr_2(PO_4)_3)^{33}$ and langbeinite-related structure (mineral langbeinite $K_2Mg_2(SO_4)_3$)^{34–39} are more appropriate for use as host matrixes that are able to encase a wide range of elements in their framework. It should be noted that the formation of Zr-containing phosphates (NZP type) takes place at temperatures higher than $1000^\circ C$.

The main purpose of the present work was to investigate the influence of potassium substitution by strontium atoms in the initial matrix $K_3Fe_2(PO_4)_3$ on the structure of complex phosphates and the founding

*Correspondence: strutyńska_n@bigmir.net

conditions for formation of Sr-containing langbeinite-related phosphates at temperatures lower than 1000 °C. For this purpose, iron was used as framework building metal, while Sr was involved by the langbeinite-type structure in the alkaline metal position. Thus, the samples of nominal composition $K_{3-2x}Sr_xFe_2(PO_4)_3$ with $x = 0.75, 1.0,$ or 1.25 and phosphate $K_3Fe_2(PO_4)_3$ were fabricated using a solid-state reaction and investigated by powder X-ray diffraction (XRD), Fourier transform infrared (FTIR) spectroscopy, and differential thermal analysis (DTA) and thermogravimetric (TG) methods.

The optimized conditions of formation of Sr-containing phosphates might be useful for the development of materials for solidification of radionuclides, such as strontium and many others.

2. Results and discussion

2.1. Powder X-ray diffraction

According to the powder XRD data, the prepared $K_3Fe_2(PO_4)_3$ belongs to a monoclinic system, space group $C2/c$ with calculated cell parameters $a = 16.293$ (2), $b = 9.468$ (2), $c = 16.704$ (2) Å, and $\beta = 118.5$ (1)°, which are close to corresponding values from the literature⁴⁰ (Figure 1a).

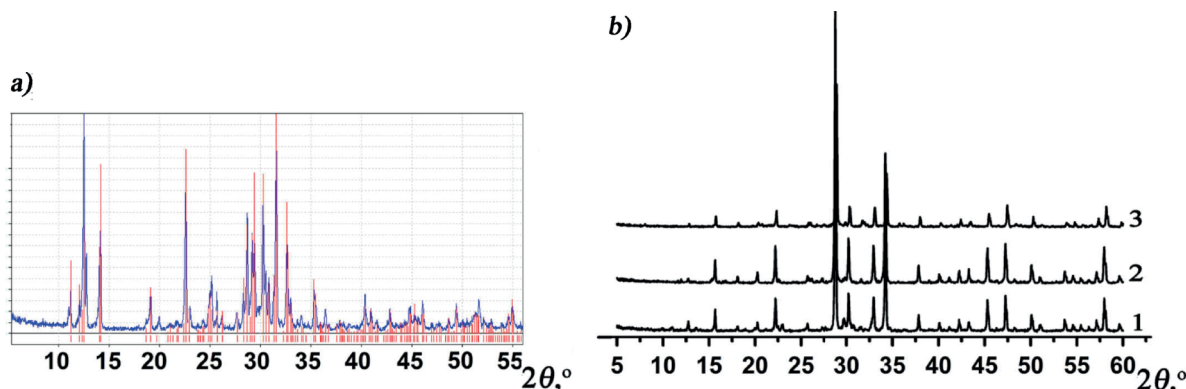


Figure 1. Powder XRD patterns for synthesized samples: a) $K_3Fe_2(PO_4)_3$ (blue color, ICDD, #00-076-1628 - red color); b) $K_{3-2x}Sr_xFe_2(PO_4)_3$ ($x = 0.75$ (curve 1), 1.0 (curve 2), and 1.25 (curve 3)).

At the same time, the XRD results for samples with compositions $KSrFe_2(PO_4)_3$ and $K_{0.5}Sr_{1.25}Fe_2(PO_4)_3$ showed the formation of single-phase langbeinite-type phosphates (Figure 1b). These compounds crystallize in the cubic system (space group $P2_13$) and calculated lattice parameters depend on their composition (Table 1). Thus, increase of the Sr amount in the phosphate caused the decreasing of parameter a , which correlates with substitution of potassium atoms by smaller strontium atoms. In the case of the sample with predictable composition $K_{1.5}Sr_{0.75}Fe_2(PO_4)_3$, a mixture of langbeinite-type phase (cubic system, space group $P2_13$, $a = 9.798$ (8) Å) and minor amount of $K_3Fe_2(PO_4)_3$ was obtained (Figure 1b). This indicates that the partial substitution of potassium atoms by strontium atoms according to $1.5 K^+ \rightarrow 0.75 Sr^{2+}$ in the $K_3Fe_2(PO_4)_3$ matrix changed the general principle of structure formation of complex phosphate with langbeinite-type framework. Thus, the early reported results showed that the $K_3Fe_2(PO_4)_3$ structure contains PO_4 -tetrahedra, FeO_6 -octahedra, and FeO_5 -polyhedra linked by common corners and forming a 3D network where the K^+ ions occupy four different positions.⁴⁰ According to the reported data,⁴¹ the phosphate $KSrFe_2(PO_4)_3$ belongs to the langbeinite family of compounds. Its crystal structure consists of a 3D framework resulting from corner-sharing between FeO_6 -octahedra and PO_4 -tetrahedra. This framework delimits two distinct cavities, statistically occupied by the K^+

and Sr^{2+} ions.⁴¹ Taking this into account, the substitution $2.5 \text{K}^+ \rightarrow 1.25 \text{Sr}^{2+}$ caused the formation also of the langbeinite-type structure that contains vacancies in the potassium positions.

Table 1. Calculated lattice parameters for obtained langbeinite-related phosphates (cubic system, space group $P2_13$).

Phosphate	a , Å
$\text{KSrFe}_2(\text{PO}_4)_3$	9.784(5)
$\text{K}_{0.5}\text{Sr}_{1.25}\text{Fe}_2(\text{PO}_4)_3$	9.769(9)

Thus, the obtained phosphates contain up to 21.0% (wt.) Sr, which indicates a perspective for the use of a langbeinite-related matrix for the bonding of Sr. It should be noted that with the aim of preparing phosphate $\text{Sr}_{1.5}\text{Fe}(\text{PO}_4)_3$ the mixture of phosphates was obtained. The main component of such mixture obtained at 1000 °C was whitlockite-related phosphate $\text{Sr}_9\text{Fe}(\text{PO}_4)_7$. The further increasing of temperature to 1080 °C and duration of sintering did not change the phase composition of obtained sample. This result indicates the important role of the potassium atom in the formation of the langbeinite-type structure.

2.2. Fourier transform infrared spectroscopy

The presence of orthophosphate anions in the prepared compounds was confirmed by the FTIR spectroscopy (Figures 2a and 2b). The bands in the region of $900\text{--}1200 \text{ cm}^{-1}$ are assigned to the stretching asymmetric and symmetric vibrations of PO_4 -tetrahedra (Figures 2a and 2b). Bands at $400\text{--}650 \text{ cm}^{-1}$ correspond to the bending vibrations. In the case of $\text{K}_3\text{Fe}_2(\text{PO}_4)_3$ (Figure 2a), the complex character of the spectrum in the region of $900\text{--}1200 \text{ cm}^{-1}$ is caused by the presence of three types of phosphorus atoms in its structure. It should be noted that the general view of spectra for the prepared samples with composition $\text{K}_{3-2x}\text{Sr}_x\text{Fe}_2(\text{PO}_4)_3$ with $x = 0.75, 1.0$, and 1.25 (Figure 2b) is typical for langbeinite-related complex phosphates.^{34–37}

2.3. Thermogravimetric and differential thermal analysis

TG and DTA results for the samples with predictable composition $\text{K}_{1.5}\text{Sr}_{0.75}\text{Fe}_2(\text{PO}_4)_3$ containing langbeinite-type phase and minor amount of $\text{K}_3\text{Fe}_2(\text{PO}_4)_3$ and pure phosphates $\text{KSrFe}_2(\text{PO}_4)_3$, $\text{K}_{0.5}\text{Sr}_{1.25}\text{Fe}_2(\text{PO}_4)_3$,

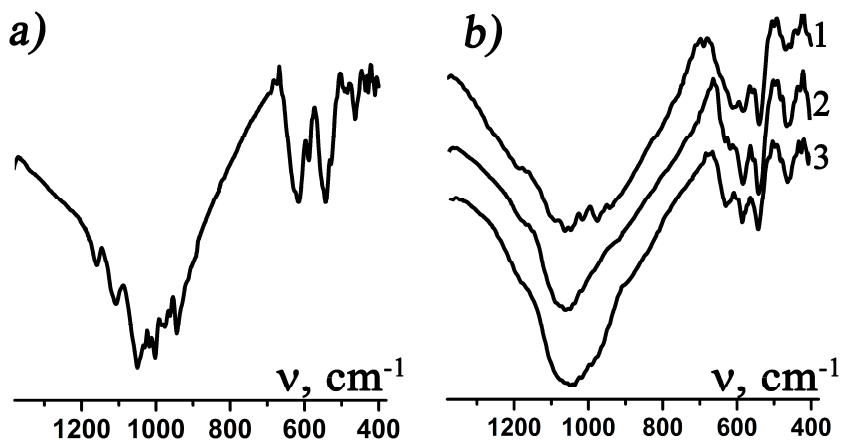


Figure 2. FTIR spectra for obtained phosphates: a) $\text{K}_3\text{Fe}_2(\text{PO}_4)_3$; b) $\text{K}_{3-2x}\text{Sr}_x\text{Fe}_2(\text{PO}_4)_3$ ($x = 0.75$ (curve 1), 1.0 (curve 2), and 1.25 (curve 3)).

and $\text{K}_3\text{Fe}_2(\text{PO}_4)_3$ are shown in Figures 3a–3d. It was found that melting points and temperatures of phosphate crystallization depend on their composition (Table 2; Figures 3a–3d). The most stable is phosphate $\text{KSrFe}_2(\text{PO}_4)_3$ with melting point at more than 1100 °C (Figure 3b), while $\text{K}_3\text{Fe}_2(\text{PO}_4)_3$ melts at 800 °C (Figure 3d), which is significantly less than corresponding values for Sr-containing phosphates (Figure 3a–3c). In the case of the sample with predictable composition $\text{K}_{1.5}\text{Sr}_{0.75}\text{Fe}_2(\text{PO}_4)_3$, the melting point of the langbeinite-type phase is at 1084 °C while a wide endothermic DTA peak confirms the presence of impurity $\text{K}_3\text{Fe}_2(\text{PO}_4)_3$ (Figure 3a).

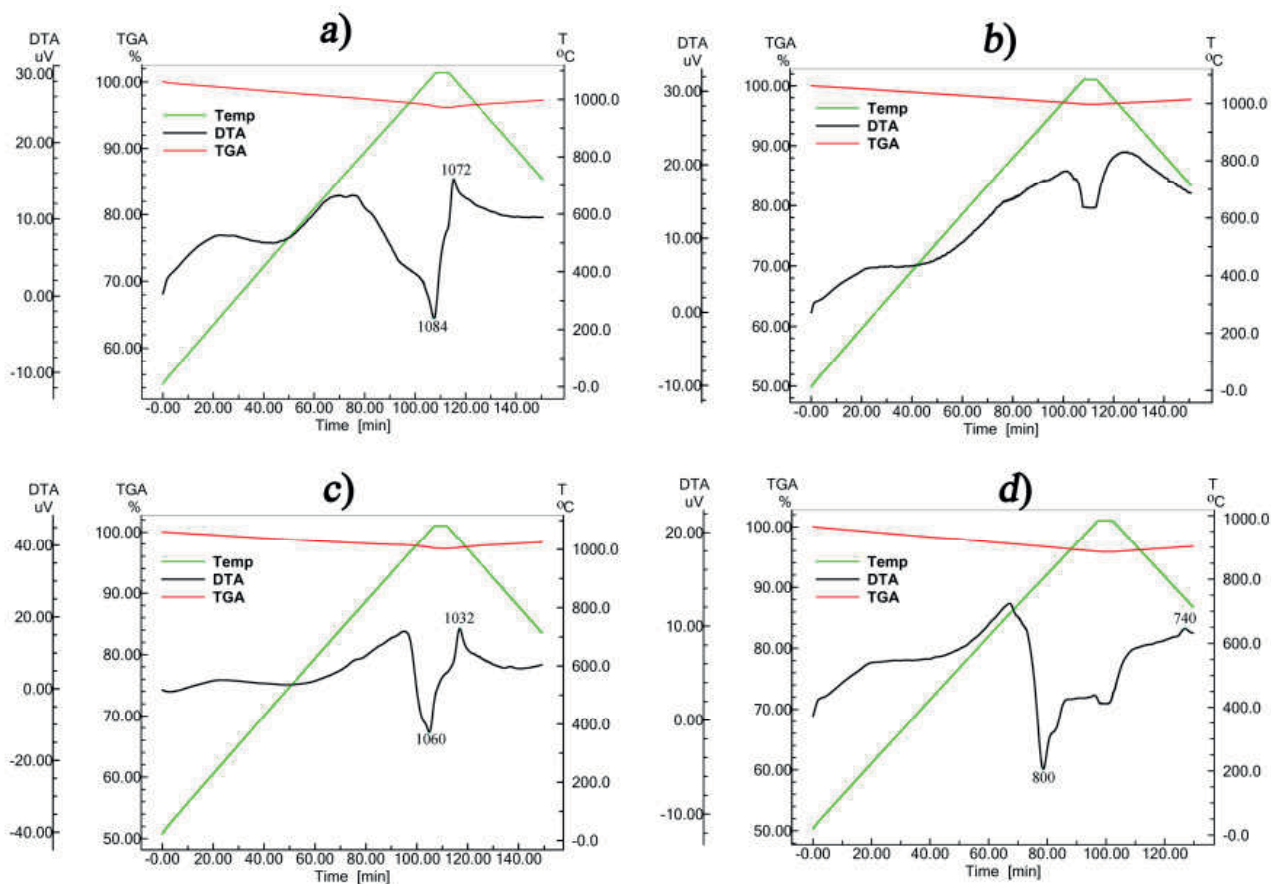


Figure 3. Thermogravimetric and differential thermal analysis for prepared phosphates $\text{K}_{3-2x}\text{Sr}_x\text{Fe}_2(\text{PO}_4)_3$ ($x = 0.75, 1.0, \text{ and } 1.25$) and $\text{K}_3\text{Fe}_2(\text{PO}_4)_3$.

Table 2. The melting points ($T_{melt.}$) and temperatures of crystallization ($T_{cryst.}$) for obtained samples with composition $\text{K}_{3-2x}\text{Sr}_x\text{Fe}_2(\text{PO}_4)_3$ ($x = 0.75, 1.0, \text{ and } 1.25$).

Composition of sample	$T_{melt.}$, °C	$T_{cryst.}$, °C
$\text{K}_{1.5}\text{Sr}_{0.75}\text{Fe}_2(\text{PO}_4)_3$	1084	1072
$\text{KSrFe}_2(\text{PO}_4)_3$	>1100	-
$\text{K}_{0.5}\text{Sr}_{1.25}\text{Fe}_2(\text{PO}_4)_3$	1061	1032

It should be noted that all prepared phosphates melt without decomposition. There are no phase transitions in the determined temperature range from 25 to 1100 °C.

2.4. Conclusions

The strontium-containing langbeinite-related phosphates $K_{3-2x}Sr_xFe_2(PO_4)_3$ ($x = 1.0$ and 1.25) have been prepared by solid-state reaction method. It was found that partial substitution $1.5 K^+ \rightarrow 0.75 Sr^{2+}$ in the initial matrix $K_3Fe_2(PO_4)_3$ led to change of the structure type with formation of langbeinite-type phase and minor amount of $K_3Fe_2(PO_4)_3$. According to TG/DTA analysis, the melting points of $K_3Fe_2(PO_4)_3$ and langbeinite-related phases are at temperatures of 800 °C and more than 1000 °C, respectively. Calculation of lattice parameters for prepared langbeinite-related phosphates has shown that strontium is crystallochemically fixed in the ceramic matrixes. The obtained results showed the influence of partial substitution of potassium by strontium in the $K_3Fe_2(PO_4)_3$ on the structure of complex phosphate that led to formation of langbeinite-type phosphate. Additionally, the key role of potassium for formation of the langbeinite-type structure in the case of phosphate $K_{0.5}Sr_{1.25}Fe_2(PO_4)_3$ was established.

It should be noted that the next stage of further investigation is the evaluation of immobilization performance for prepared phosphates and after that the development of methods for immobilization of strontium-90. The main advantages of the proposed approach of including Sr in stable iron-containing langbeinite-type matrixes are synthesis time reduction (to 8 h) and temperature reduction (to 900 °C) as compared to the use of zirconium-containing NZP ceramics for this purpose (pure NZP phases were obtained during sintering at 1250 °C for 72 h).

3. Experimental

3.1. Synthesis of phosphates

The samples of nominal composition $K_{3-2x}Sr_xFe_2(PO_4)_3$ with $x = 0.75, 1.0,$ or 1.25 and phosphate $K_3Fe_2(PO_4)_3$ were prepared by conventional solid-state reaction method. All initial components KH_2PO_4 , Fe_2O_3 , $(NH_4)_2HPO_4$, and $Sr(NO_3)_2$ were of analytical grade (more than 99.9%, Merck). Stoichiometric quantities of initial materials were ground well in an agate mortar and initially heated to 500 °C for 4 h for removal of volatile products. The obtained powders were reground and sintered in a platinum crucible at 750 °C (for all samples) and higher temperature in the range of 870–900 °C depending on the composition of phosphate.

3.2. Characterization of prepared phosphates

The phase composition of the prepared samples was determined using powder XRD. A Shimadzu XRD-6000 diffractometer with CuK_α radiation (graphite counter monochromator) was used. Data were collected over the 2θ range of 5° to 60° with a step of 0.02° at a fixed counting time of 3 s/step. The identification of phases was achieved by comparing the diffraction patterns of the prepared powders with the standards of the International Centre for Diffraction Data (ICDD). The identification card numbers of reference XRD patterns for $K_3Fe_2(PO_4)_3$ and langbeinite-related phosphates were #00-076-1628 and #01-089-6891, respectively. The FullProf program was used for calculation of lattice parameters.

To confirm the anion type of phosphates, their FTIR spectra were recorded using a PerkinElmer Spectrum BX spectrometer in the range of 400–4000 cm^{-1} at 1 cm^{-1} resolution for the samples pressed into pellets of KBr.

The thermal stability of obtained phosphates was investigated using Shimadzu simultaneous TGA/DTA analyzer DTG-60H. The compounds were heated in a platinum crucible in air atmosphere with a rate 10 °C/min from room temperature to 1100 °C and kept for 30 min at this temperature followed by cooling to 700 °C at the same rate. α -Al₂O₃ was used as a standard sample.

References

1. Jedinakova-Krizova, V. *J. Radioanal Nucl Ch.* **1998**, *229*, 13-18.
2. Gennaro, B.; Colella, A.; Aprea, P.; Colella, C. *Micropor. Mesopor. Mat.* **2003**, *61*, 159-165.
3. Pabalan, R. T.; Bertetti, F. P. In: *Cation-Exchange Properties of Natural Zeolites*; Bish, D. L.; Ming, D. W., Eds. Mineralogical Society of America: Washington, DC, USA, 2001, pp. 453-518.
4. Chelishchev, N. F. In: Ming, D. W.; F.A. Mumpton, F. A., Eds. *Natural Zeolites '93*; International Committee on Natural Zeolites: Brockport, NY, USA, 1995, pp. 525-532.
5. Cappelletti, P.; Rapisardo, G.; Gennaro, B. *J. Nucl. Mater.* **2011**, *414*, 451-457.
6. Plodinec, M. J. *Glass Technol.* **2000**, *41*, 186-192.
7. Kim, M.; Heo, J. *J. Nucl. Mater.* **2015**, *467*, 224-228.
8. Sales, B. C.; Boatner, L. A. *Mater. Lett.* **1984**, *2*, 301-304.
9. Ojovan, M.; Lee, W. *Metall. Mater. Trans. A* **2011**, *42*, 837-851.
10. Gin, S.; Abdelouas, A.; Criscenti, L. J.; Ebert, W. L.; Ferrand, K.; Geisler, T.; Harrison, M. T.; Inagaki, Y.; Mitsui, S.; Mueller, K. T. et. al. *Mater. Today* **2013**, *16*, 243-248.
11. Donald, I. W.; Metcalfe, B. L.; Fong, S. K.; Gerrard, L. A.; Strachan, D. M.; Scheele, R. D. *J. Nucl. Mater.* **2007**, *361*, 78-93.
12. He, Y.; Bao, W.; Song, C. *J. Nucl. Mater.* **2002**, *305*, 202-208.
13. Huang, Y.; Zhang, H.; Zhou, X.; Peng, S. *J. Nucl. Mater.* **2017**, *485*, 105-112.
14. Clavier, N.; Podor, R.; Dacheux, N. *J. Eur. Ceram. Soc.* **2011**, *31*, 941-976.
15. Kumar, S. P.; Gopal, B. *J. Nucl. Mater.* **2015**, *458*, 224-232.
16. Meldrum, A.; Boatner, L. A.; Weber, W. T.; Ewing, R. C. *Geochim. Cosmochim. Ac.* **1998**, *62*, 2509-2520.
17. Dacheux, N.; Clavier, N.; Podor, R. *Am. Mineral.* **2013**, *98*, 833-847.
18. Clavier, N.; Dacheux, N.; Podor, R. *Inorg. Chem.* **2006**, *45*, 220-229.
19. Orlova, A. I.; Orlova, M. P.; Solov'eva, E. M.; Loginova, E. E.; Demarin, V. T.; Kazantsev, G. N.; Samoilov, S. G.; Stefanovskii, S. V. *Radiochemistry* **2006**, *48*, 561-567.
20. Orlova, A. I. *Radiochemistry* **2002**, *44*, 423-445.
21. Nakayama, S.; Itoh, K. *J. Eur. Ceram. Soc.* **2003**, *23*, 1047-1052.
22. Haik, A. H.; Deb, S. B.; Chalke, A. B.; Saxena, M. K.; Ramakumar, K. L.; Venugopal, V.; Dharwadkar, S. R. *J. Chem. Sci.* **2010**, *122*, 71-82.
23. Gregg, D. J.; Karatchevtseva, I.; Triani, G.; Lumkin, G. R.; Vance, E. R. *J. Nucl. Mater.* **2013**, *441*, 203-210.
24. Scheetz, B. E.; Agrawal, D. K.; Breval, E.; Roy, R. *Waste Manage.* **1994**, *14*, 489-505.
25. Gregg, D. J.; Karatchevtseva, I.; Thorogood, G. J.; Davis, J.; Bell, B. D. C.; Jackson, M.; Dayal, P.; Ionescu, M.; Triami, G.; Short, K. et al. *J. Nucl. Mater.* **2014**, *446*, 224-231.
26. Orlova, A. I.; Volgutov, V. Yu.; Mikhailov, D. A.; Bykov, D. M.; Skuratov, V. A.; Chuvil'deev, V. N.; Nokhrin, A. V.; Boldin, M. S.; Sakharov, N. V. *J. Nucl. Mater.* **2014**, *446*, 232-239.

27. Pet'kov, V.; Asabina, E.; Loshkarev, V.; Sukhanov, M. *J. Nucl. Mater.* **2016**, *471*, 122-128.
28. Bohre, A.; Shrivastava, O. P. *J. Nucl. Mater.* **2013**, *433*, 486-493.
29. Kumar, S.; Gopal, B. *J. Alloy Comp.* **2016**, *657*, 422-429.
30. Kumar, S. P.; Gopal, B. *J. Alloy Comp.* **2014**, *615*, 419-423.
31. Dacheux, N.; Clavier, N.; Robisson, A. C.; Terra, O.; Audubert, F.; Lartigue, J.; Guy, C. *Chimie* **2004**, *7*, 1141-1152.
32. Terra, O.; Dacheux, N.; Audubert, F.; Podor, R. *J. Nucl. Mater.* **2006**, *352*, 224-232.
33. Shrivastava, O. P.; Chourasia, R. *J. Hazard. Mater.* **2008**, *153*, 285-292.
34. Ogorodnyk, I. V.; Zatoovsky, I. V.; Slobodyanik, N. S.; Baumer, V. N.; Shishkin, O. V. *J. Solid State Chem.* **2006**, *179*, 3461-3466.
35. Strutynska, N. Y.; Bondarenko, M. A.; Ogorodnyk, I. V.; Zatoovsky, I. V.; Slobodyanik, N. S.; Baumer, V. N.; Puzan, A. N. *Cryst. Res. Technol.* **2015**, *50*, 549-555.
36. Ogorodnyk, I. V.; Zatoovsky, I. V.; Baumer, V. N.; Slobodyanik, N. S.; Shishkin, O. V.; Vorona, I. P. *J. Solid State Chem.* **2007**, *180*, 2838-2844.
37. Zatoovsky, I. V.; Slobodyanik, N. S.; Ushchapivskaya, T. I.; Ogorodnyk, I. V.; Babaryk, A. A. *Russ. J. Appl. Chem.* **2006**, *79*, 10-15.
38. Strutynska, N. Y.; Bondarenko, M. A.; Ogorodnyk, I. V.; Baumer, V. N.; Slobodyanik, N. S.; Brown, I. D. *Acta Crystallogr. E* **2015**, *E71*, 251-253.
39. Babaryk, A. A.; Zatoovsky, I. V.; Slobodyanik, N. S.; Ogorodnyk, I. V. *Z. Naturforsch.* **2008**, *B63*, 345-348.
40. Pintard-Screpel, P. M.; D'Yvoire, F. *Acta Crystallogr. C* **1983**, *C39*, 9-12.
41. Hidouri, M.; López, M. L.; Pico, C.; Wattiaux, A.; Ben Amara, M. *J. Mol. Struct.* **2012**, *1030*, 145-148.